catalysts

MDPI

Supplementary Information

Cu modified TiO_2 catalyst for electrochemical reduction of carbon dioxide to methane

Akihiko Anzai[1], Ming-Han Liu,[1] Kenjiro Ura [2], Tomohiro G Noguchi,[1] Akina Yoshizawa,[1] Kenichi Kato [3], Takeharu Sugiyama [4] and Miho Yamauchi [1,5,6,7,*]

*Correspondence to yamauchi@ms.ifoc.kyushu-u.ac.jp

1 International Institute for Carbon-Neutral Energy Research (WPI-I²CNER), Kyushu University, 744 Motooka, Nishi-ku Fukuoka 819-0395, Japan.

2 Department of Chemistry, Graduate School of Science, Kyushu University, 744 Motooka, Nishi-ku Fukuoka 819-0395, Japan.

3 RIKEN SPring-8 Center, 1-1-1 Kouto, Sayo-cho, Sayo-gun, Hyogo, 679-5148, Japan.

4 Research Center for Synchrotron Light Applications, Kyushu University, 6-1 Kasuga-koen, Kasuga, Fukuoka, 816–8580 Japan

5 Institute for Materials Chemistry and Engineering (IMCE), Kyushu University, 744 Motooka, Nishi-ku, Fukuoka, 819-0395, Japan

6 Advanced Institute for Materials Research(AIMR), Tohoku University, 2-1-1 Katahira, Aoba-ku, Sendai, 980-8577, Japan

7 Research Center for Negative Emissions Technologies (K-Nets), Kyushu University, Motooka 744, Nishi-ku, Fukuoka 819-0395, Japan

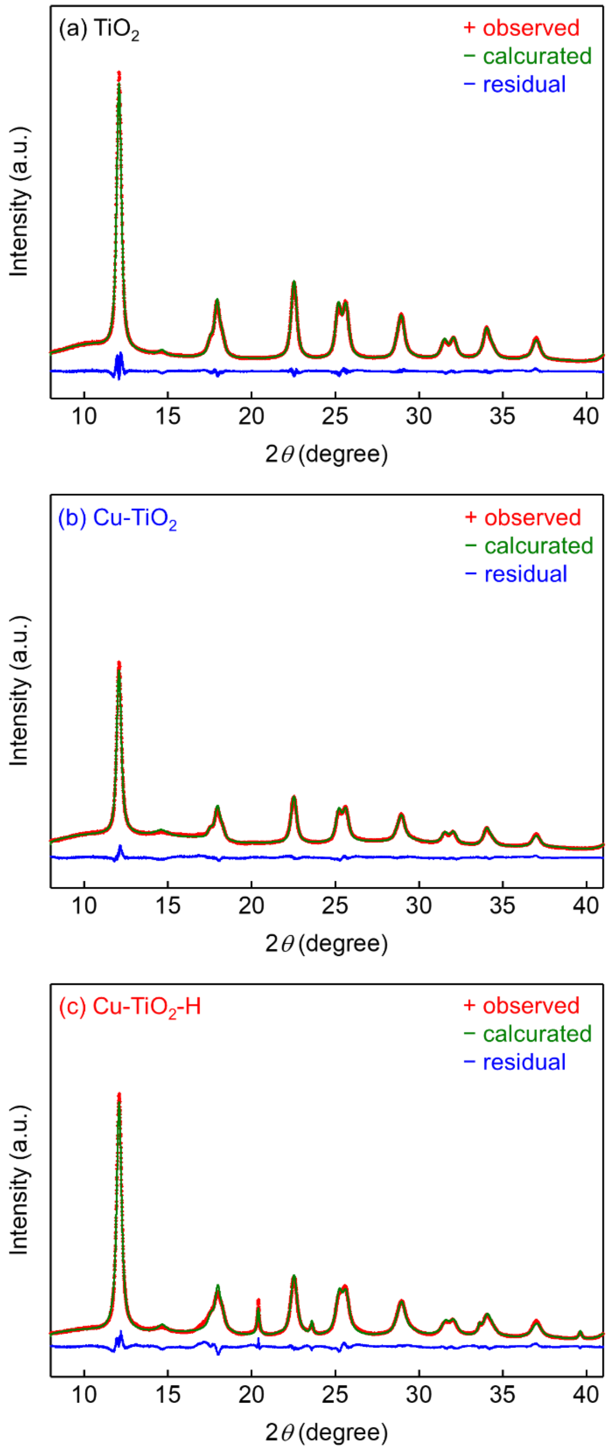

Figure S1 Rietveld analysis results for XRD pattern for (a) TiO_2, (b) Cu-TiO_2, (c) Cu-TiO_2-H. The observed diffraction intensities, calculated patterns, and the difference between the observed and calculated intensity are denoted by red plus signs, a green solid line, and a blue solid line.

Table S1 Structural parameters determined by Rietveld profile fitting for an XRD pattern of TiO_2, Cu-TiO_2 and Cu-TiO_2-H.

	TiO_2		Cu-TiO_2		Cu-TiO_2-H		
percent-age (%)	92.6	7.4	71.4	28.6	76.9	21.2	1.88

crystal system	tetragonal	orthorhombic	tetragonal	orthorhombic	tetragonal	orthorhombic	cubic
space group	I41/amd	Pbca	I41/amd	Pbca	I41/amd	Pbca	Fm-3m
a (Å)	3.78632(5)	9.061(7)	3.78784(7)	9.034(6)	3.78626(9)	9.064(7)	3.618
b (Å)	-	5.472(4)	-	5.456(3)	-	5.496(3)	-
c (Å)	9.48853(16)	5.218(4)	9.4762(2)	5.278(3)	9.4669(3)	5.196(4)	-
V (Å^3)	136.029(4)	258.7(3)	135.962(6)	260.2(3)	135.715(8)	258.8(3)	47.358(9)
T (K)	298	298	298	298	298	298	298
R_{wp}	3.18	3.18	2.97	2.97	4.39	4.39	4.39
R_{exp}	1.55	1.55	1.55	1.55	1.53	1.53	1.53
GOF	2.06	2.06	1.92	1.92	2.87	2.87	2.87
2θ range	8-110°	8-110°	8-110°	8-110°	8-110°	8-110°	8-110°
wave length (Å)	0.739606	0.739606	0.739606	0.739606	0.739606	0.739606	0.739606

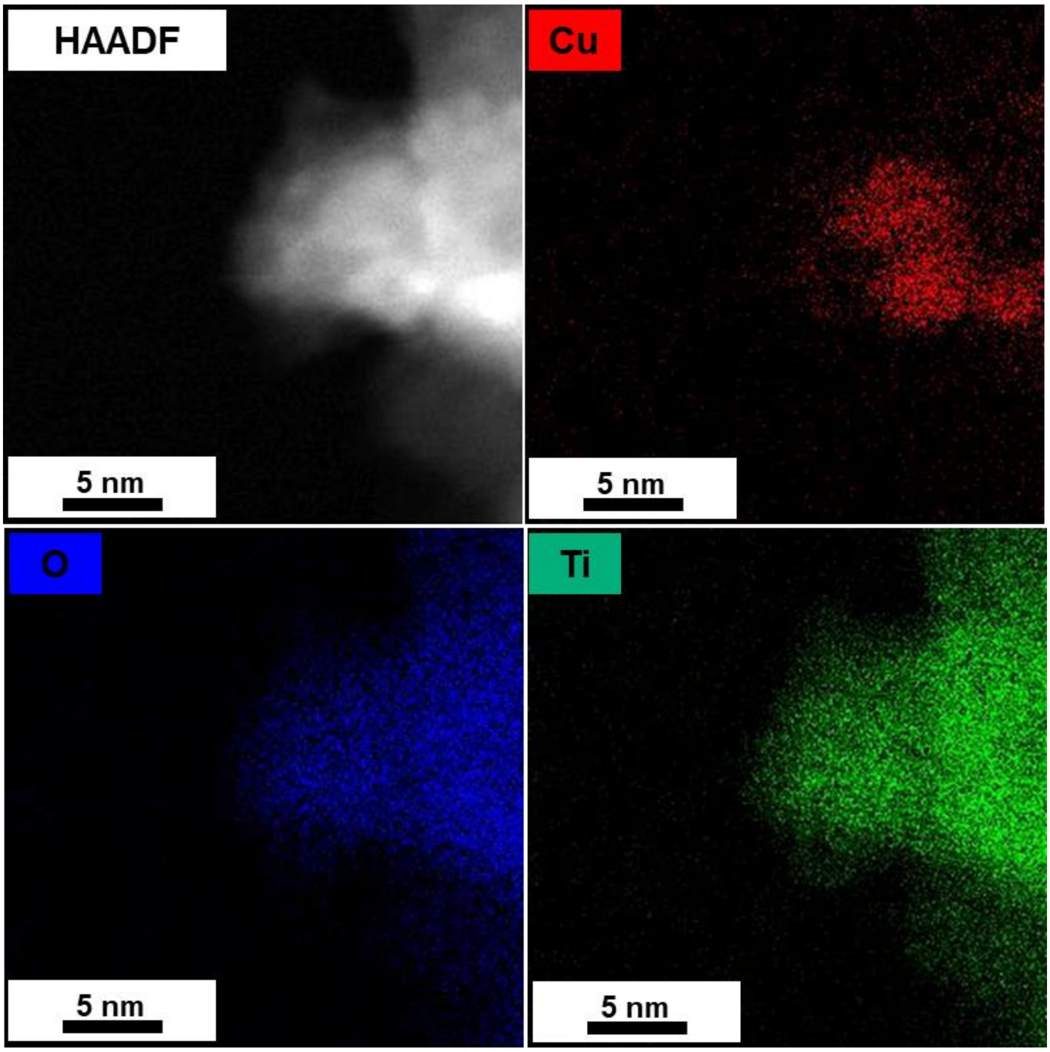

Figure S2 High-angle annular dark-field scanning transmission electron microscopy (HAADF-STEM) image and EDS mapping images of Cu-TiO_2.

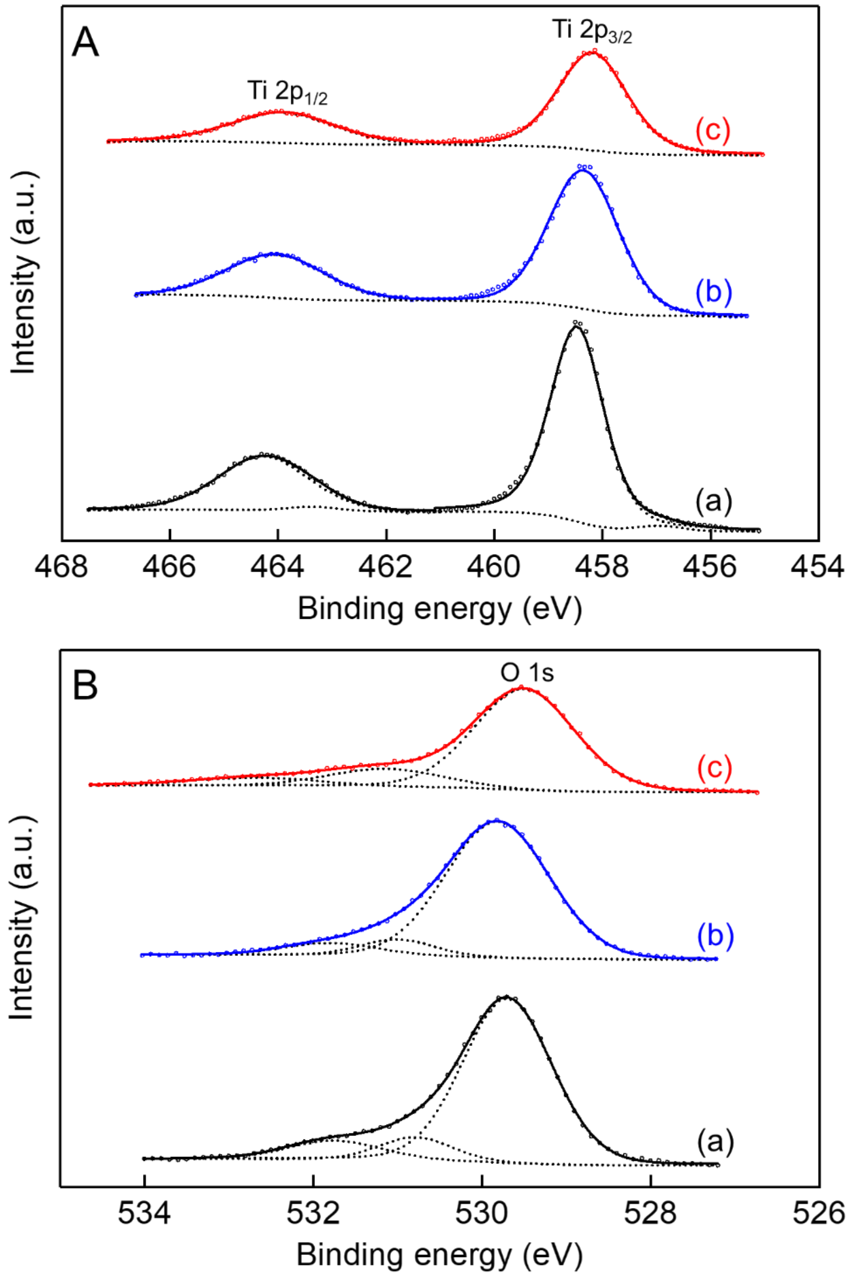

Figure S3 Deconvoluted Ti 2p (A) and O 1s (B) XPS spectra of (a) TiO_2, (b) Cu-TiO_2, and (c) Cu-TiO_2-H. The observed spectra, fitting curves and calculated patterns, and deconvoluted curves are denoted by circle, solid line, and dashed line, respectively.

Table S2 XPS peak positions and phase assignment of the TiO_2, Cu-TiO_2, and Cu-TiO_2-H samples.

sample	Binding energy (eV)		Phase assignment
TiO_2	O 1s	529.7	lattice oxygen of TiO_2
		530.8	hydroxide group or water molecules on the surface
		531.8	organic contaminants containing oxygen species

	Ti 2p 3/2	458.5	TiO_2
	Ti 2p 1/2	464.2	TiO_2
Cu-TiO_2	O 1s	529.8	lattice oxygen of TiO_2
		531.0	hydroxide group or water molecules on the surface
		531.9	organic contaminants containing oxygen species
	Ti 2p 3/2	458.3	TiO_2
	Ti 2p 1/2	464.0	TiO_2
	Cu 2p 3/2	932.3	Cu(I) and CuO
		934.3	$Cu(OH)_2$
	satellite	941.0, 943.6	Cu(II)
Cu-TiO_2-H	O 1s	529.5	lattice oxygen of TiO_2
		531.2	hydroxide group or water molecules on the surface
		532.8	organic contaminants containing oxygen species
	Ti 2p 3/2	458.1	TiO_2
	Ti 2p 1/2	463.9	TiO_2
	Cu 2p 3/2	931.9	Cu(0) and Cu(I)
		933.3	Cu(II)

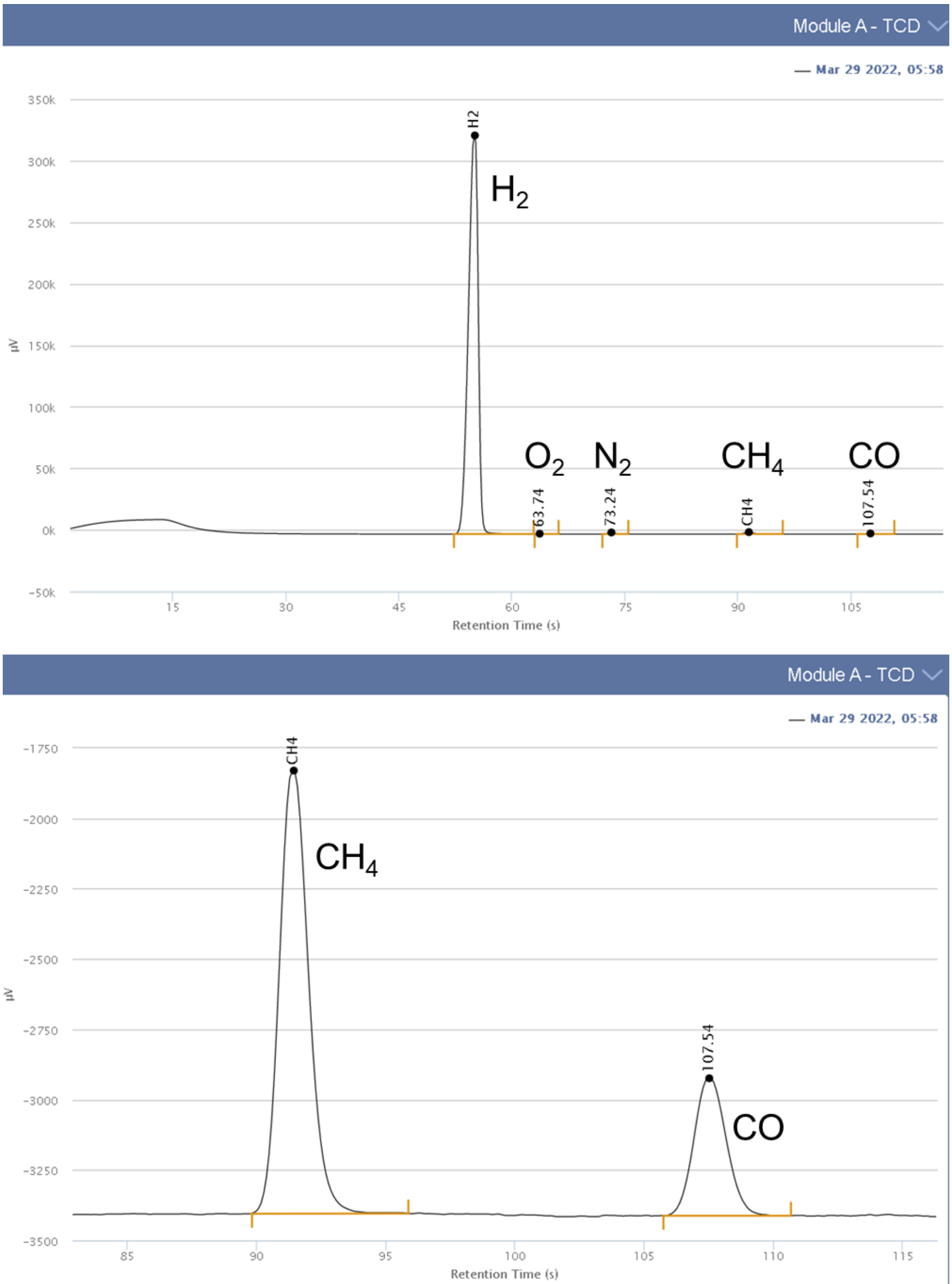

Figure S4 Example of a gas chromatogram (below: enlarged view in the region for CH_4 and CO) of H_2, CH_4, and CO obtained by electrochemical reduction of CO_2 using Cu-TiO_2-H catalyst on a Molsieve 5A column channel after chronoamperometry operation of 10 min at 1.8 V vs. RHE.

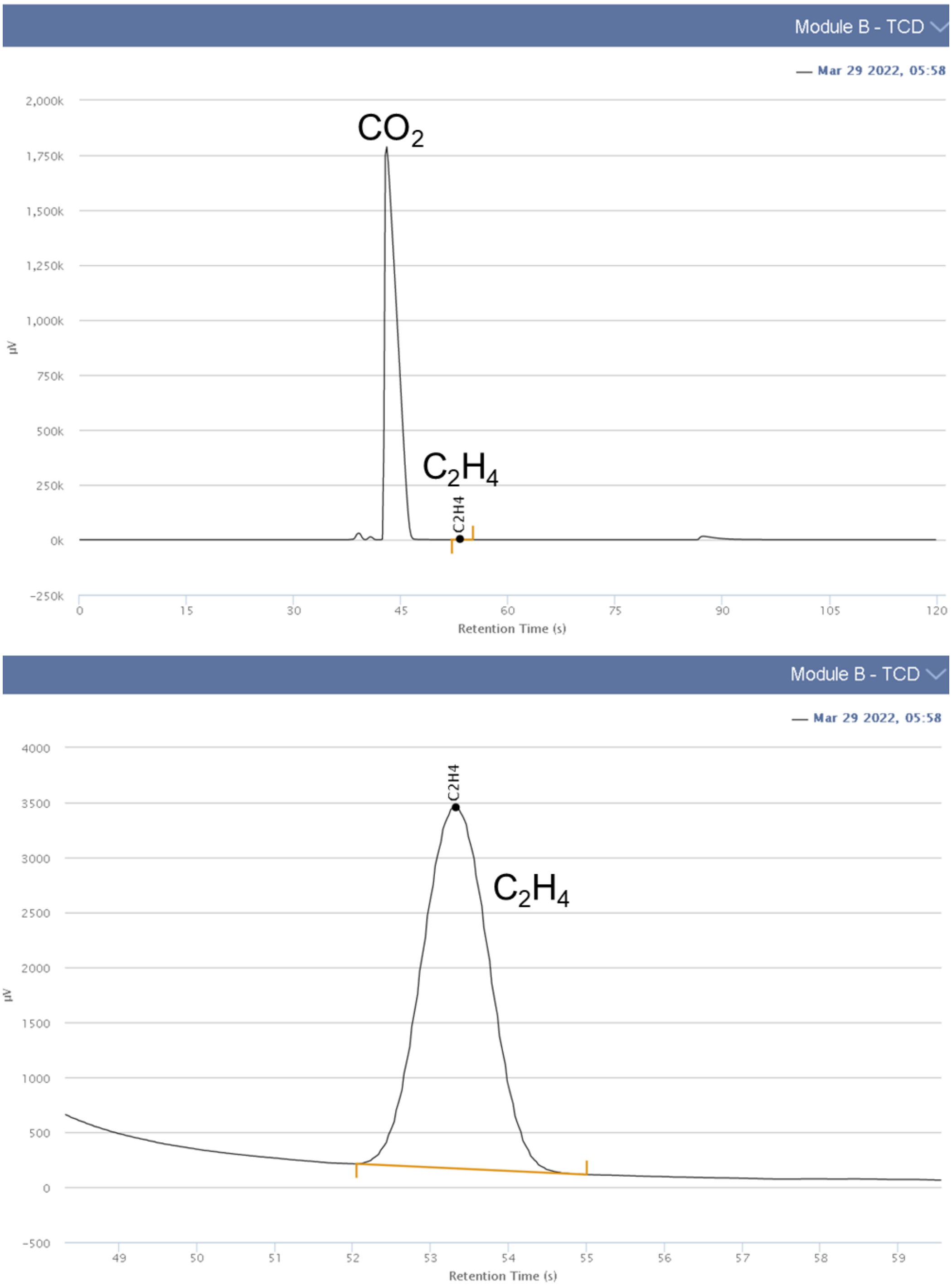

Figure S5 Example of a gas chromatogram (below: enlarged view in the region for C_2H_4) of C_2H_4 obtained by electrochemical reduction of CO_2 using Cu-TiO_2-H catalyst on a Plot Q column channel after chronoamperometry operation of 10 min at 1.8 V vs. RHE.

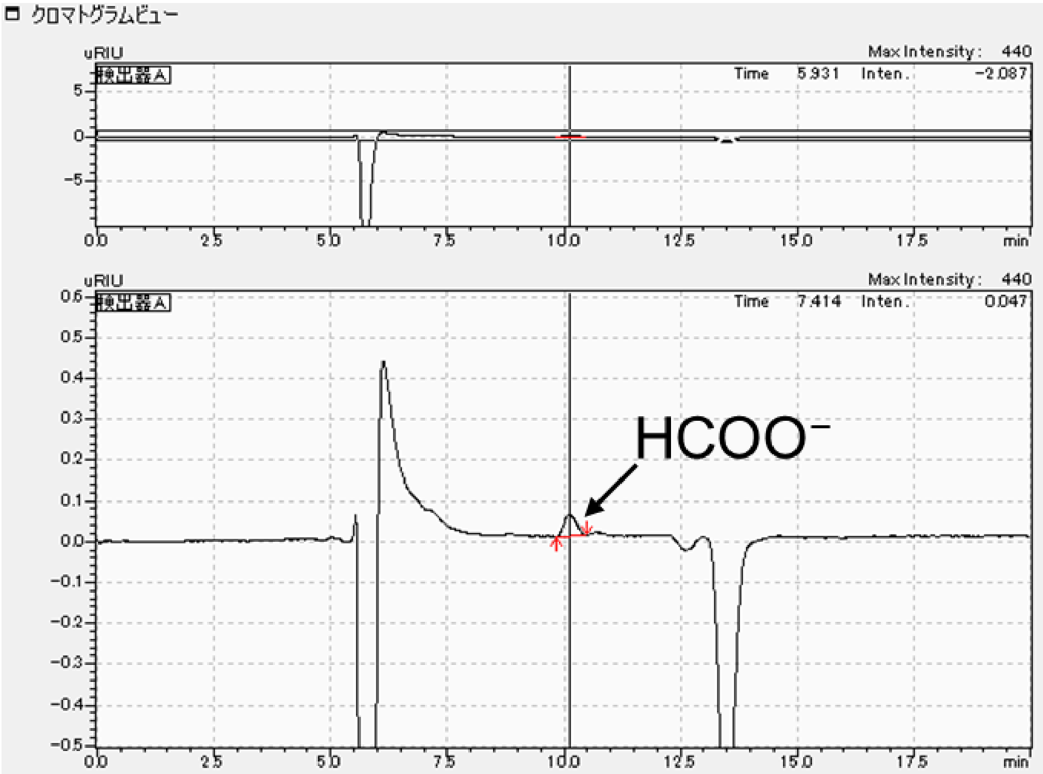

Figure S6 Example of a High Performance Liquid Chromatography (HPLC) of liquid products obtained by electrochemical reduction of CO_2 using Cu-TiO_2-H catalyst after chronoamperometry operation of 10 min at 1.8 V vs. RHE.

Table S3 Electrochemical CO_2-to-CH_4 performance for studies related to highly dispersed or single-site copper catalysts.

Catalyst	Electrolyte	Cathod potential (full cell potential) (V vs. RHE)	Partial current density for CH_4 production (mA cm^{-2})	FE (%)	FE_{CH4}/FE_{C1+C2} (%)	Ref.
Cu-TiO_2	1 M KOH	−1.8 V	36	18	70	This work
Cu-CeO_2	CO_2-saturated 0.1 M $KHCO_3$	−1.8 V	33.6	58	71	*ACS Catal.* **2018**, 8, 7113–7119.
Cu-N-5%-400	1 M KOH	−1.0 V	100	42	61	*Journal of Electroanalytical Chemistry*, **2020**, 875, 113862.
Cu-N-C-900	CO_2 saturated 0.1 M $KHCO_3$	−1.6 V	14.8	38.6	62	*ACS Energy Lett.* **2020**, 5, 1044–1053.
Cu/C-Al_2O_3	1.0 M KOH	−1.2 V	94.8	62	43	*Nano Lett.*, **2021**, 21, 7325–7331.

Cu-230/MWCNT	CO_2 saturated 0.1 M $KHCO_3$	−1.8 V	23	45	77	*ACS Sustainable Chem. Eng.* **2021**, 9, 13536–13544.